Supplementary Information for

A Diiron(IV) Complex that Cleaves Strong C-H and O-H Bonds

Dong Wang, Erik R. Farquhar, Audria Stubna, Eckard Münck,* and Lawrence Que, Jr.*

Materials and Methods

General Materials and Procedures. All chemicals are of the highest commercially available purity and were used as received, unless noted otherwise. CH_3CN and CD_3CN were distilled from CaH_2 under Ar before use. CH_3OH was distilled from Mg under Ar. CD_3OH, CH_3OD and CD_3OD were dried over molecular sieve before use. Elemental analysis was performed by Atlantic Microlab (Norcross, GA).

Ligand Synthesis. The ligand L was synthesized by a modification of a literature procedure[1]. A 250 mL round bottom flask with stir bar was charged with 2-chloromethyl-4-methoxy-3,5-dimethylpyridine hydrochloride (4.44 g, 20 mmol) dissolved in distilled H_2O (40 mL). *N*-acetylethylenediamine (1.02 g, 10 mmol) was added and formed a white precipitate immediately. The cloudy solution was cooled to 0 ^{o}C in an ice-water bath and an aqueous solution (10 mL) of 4 M NaOH was then added dropwise to form a clear solution. The solution was stirred at room temperature for 3 days under Ar and then extracted with chloroform (3 × 20 mL). After drying the organic phase over Na_2SO_4, the solvent was removed to obtain a colorless oil of L in 40%-50% yield. The oil was further purified by flash chromatography over Al_2O_3 using ethyl acetate-methanol (95 : 5) as eluant, yielding a white solid after solvent was evaporated. ^{1}H-NMR (CD_3Cl): 8.13 (s, 6-H, 2H), 3.75 (s, py-CH_2, 4H), 3.67 (s, 4-OCH_3, 6H), 3.22 (q, CH_2, 2H, *J* = 6.5 Hz), 2.71 (t, CH_2, 2H, *J* = 5.5 Hz), 2.18 (s, 3-CH_3, 6H), 2.10 (s, 5-CH_3, 6H), 1.92 (s, acetyl, 3H).

Preparation and crystallization of Diiron(III) Complex 1. L (0.40 g, 1 mmol) and $Fe(OTf)_2(CH_3CN)_2$[2] (0.44 g, 1 mmol) were dissolved in 10 mL acetonitrile to form a red solution. Triethylamine (0.10 g, 1 mmol, 0.14 mL) was then added to yield a dark brown solution. Addition of diethyl ether into the solution affords a brown solid

[Fe$^{III}_2$O(L)$_2$](OTf)$_2$•2H$_2$O (**1-OTf**). Anal. for C$_{46}$H$_{66}$Fe$_2$O$_{15}$N$_8$S$_2$F$_6$ Calcd (Found): C, 43.81 (43.63); H, 5.24 (5.15); N, 8.80 (8.38); S, 5.18 (5.53). The ^{57}Fe-enriched complex was prepared analogously by using ^{57}Fe(OTf)$_2$(CH$_3$CN)$_2$. To grow crystals of **1** suitable for X-ray crystallography, **1-OTf** (0.0126 g, 0.01 mmol) was dissolved in 1 mL methanol, and 1 eq NaBPh$_4$ (pre-dissolved in methanol) was then added to yield a brown precipitate. The precipitate was filtered, washed with methanol and re-dissolved into a 1 mL mixture of 1:1 acetonitrile and methanol. Dark brown crystals of [Fe$^{III}_2$O(L)$_2$](BPh$_4$)$_2$ (**1-BPh$_4$**) were obtained by slow volatilization of acetonitrile then charged for X-ray crystallography characterization.

Physical Methods. UV-vis spectra were recorded with a Hewlett-Packard 8453A diode array spectrometer equipped with a Unisoku Scientific Instruments cryostat (Osaka, Japan) for temperature control. ^{1}H NMR spectra were recorded on a Varian Inova VI-500 spectrometer at ambient temperature. Chemical shifts (ppm) were referenced to the residual solvent peaks. Cyclic voltammetry (CV) and controlled potential bulk electrolysis were performed on a CS-1200 Computer-Controlled Potentiostat Electroanalytical System from Cypress Systems, Inc. (Lawrence, Kansas) in dry CH$_3$CN and CD$_3$CN with 0.10 M potassium hexaflurophosphate (KPF$_6$) as supporting electrolyte on a standard three electrode cell. Constant acceleration Mössbauer spectrometers, equipped with Janis SuperVaritemp cryostats, were used to collect spectra in magnetic fields up to 8.0 T, which were applied parallel to the observed γ-radiation. Data were analyzed with the software WMOSS (WEB Research, Edina, MN), and isomer shifts are reported relative to Fe-metal at 295 K. X-ray absorption spectra were measured on beamlines 7-3 and 9-3 at the Stanford Synchrotron Radiation Lightsource (SSRL) with the storage ring operating at 3 GeV and 80-100 mA. Fe K-edge XAS data were collected for frozen solutions maintained at ~ 10 – 15 K over an energy range of 6.9 – 8.0 keV using a Si(220) monochromator for energy selection and an Oxford Instruments CF1208 continuous flow liquid helium cryostat for temperature control. A Rh-coated mirror upstream of the monochromator was used for harmonic rejection. Data were obtained as fluorescence excitation spectra with a 30 element solid-state germanium detector array (Canberra). An iron foil spectrum was recorded concomitantly for internal

energy calibration and the first inflection point of the K-edge was assigned to 7112.0 eV. Data reduction, averaging, and normalization were performed using the program EXAFSPAK[3], using a previously defined protocol[4]. Analysis of the pre-edge features was carried out with the program SSExafs[5] using an established methodology[6]. In all fits, the coordination number n of a given shell was a fixed parameter, and was varied iteratively while r and σ^2 were allowed to freely float. The scale factor S_0 was fixed at 0.9, while the edge shift parameter E_0 was allowed to float as a common value for all shells. Phase and amplitude parameters for a given absorber-scatterer pair at a defined distance were calculated using FEFF at the single-scattering level of theory, and utilized by the 'opt' program of the EXAFSPAK package during curve-fitting. For purposes of quantifying fit quality, the goodness-of-fit parameter F was defined as $[\Sigma k^6(\chi_{exptl}-\chi_{calc})^2 / \Sigma k^6 \chi_{exptl}^2]^{1/2}$. GC and GC-MS analysis was carried out on an AutoSystem XL GC from PerkinElmer Instruments LLC (Shelton, Connecticut) and a Finnigan MAT 95 mass spectrometer attached with a Hewlett-Packard Series II Model 5890 GC.

Kinetic Studies and Product Analysis. C-H and O-H bond reactivity studies were carried out at 10 ^{o}C under Ar unless otherwise stated. For a typical experiment, the substrate of an excess amount was injected into a 1 cm pathlength UV cuvette containing freshly prepared solution of **3**. The reaction was monitored by UV-vis spectroscopy following the absorption change at 680 nm. The time traces were fitted to a pseudo-first-order mode to obtain k_{obs} values. After the reaction was completed, 1.1 equivalents ferrocene were added to fully reduce the formed **2**. Product analysis was carried out either by GC and GC-MS (for cyclohexane reactions, naphthalene as the internal standard), or by ^{1}H NMR spectroscopy (for cyclohexene, 1,3-cyclohexadiene and *tert*-butanol reactions, benzene as the internal standard). For cyclohexane and *tert*-butanol reactions, iron-containing complexes were first removed by passing the reaction solutions through a basic Al_2O_3 flash column. A small amount of dry CD_3CN was then used to elute the residual organic compounds out. For cyclohexene and 1,3-cyclohexadiene reactions, the oxidant:substrate ratio was varied from 1:2 to 1:10. ^{1}H NMR spectra were recorded *in situ* without removing iron-containing complexes. Several blank control experiments including solvent, substrate, self-decay of **3**,

ferrocene and internal standards were carefully performed to ensure that the reaction of **3** with substrates is the unique way to give the target products.
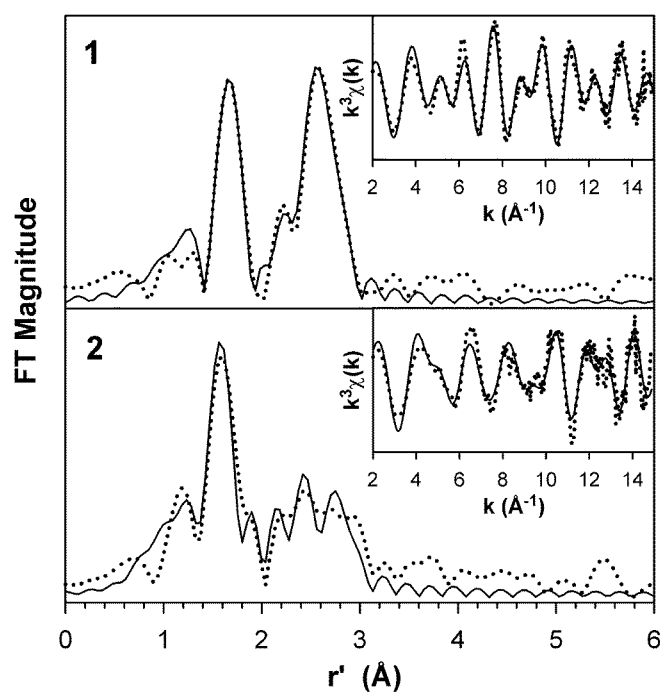
**Fig. S1.** Fourier transforms of the Fe K-edge EXAFS data ($k^3\chi(k)$) and unfiltered EXAFS spectra ($k^3\chi(k)$, inset) of **1** (top) and **2** (bottom). Experimental data is shown with dotted (······) lines and fits with solid (——) lines. Fourier transformation range, k = 2.0 – 15.0 Å^{-1} (**1**) or 2.0 – 14.9 Å^{-1} (**2**). Fit parameters are shown in bold italics in Table S2 for **1** and Table S3 for **2**.
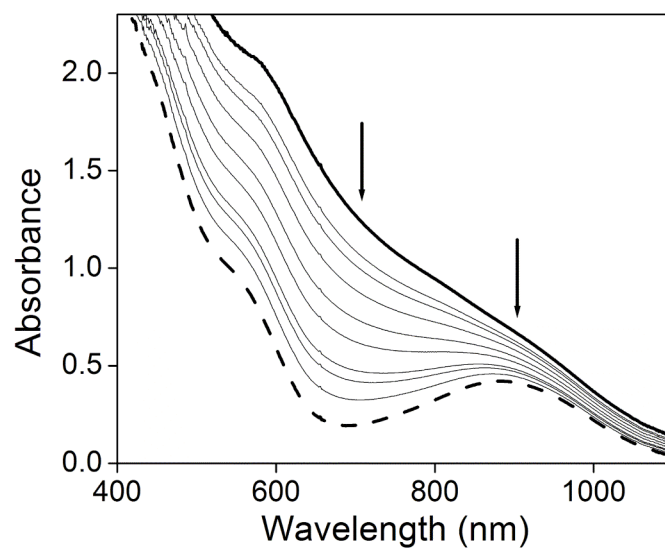
Fig. S2. Reduction of 0.5 mM **3** (solid line) to **2** (dashed line) by 0.1 M cyclohexane at 10 °C in CD_3CN. Arrows indicate the spectral changes during the reaction.
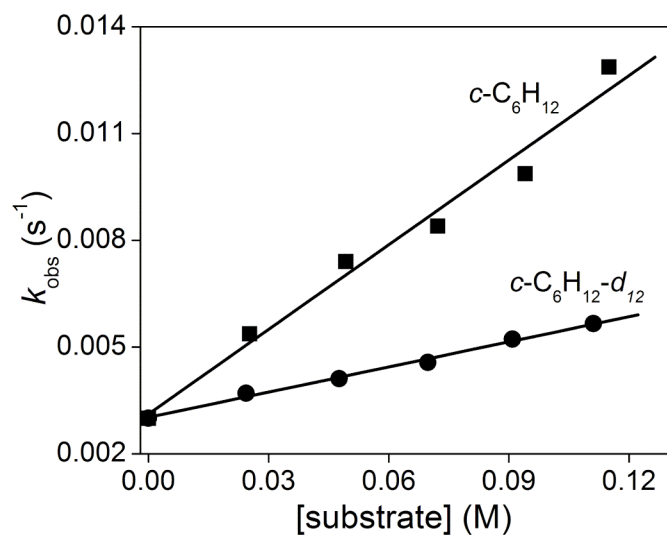
Fig. S3. Plots of the substrate concentration dependence of the pseudo-first-order rate constants for the oxidation of (■) c-C_6H_{12} and (●) c-C_6H_{12}-d_{12} at 10 °C in CD$_3$CN.
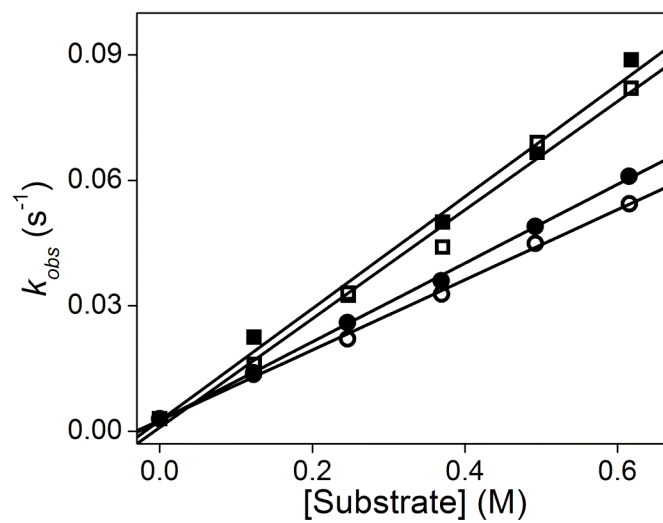
Fig. S4. Plots of the substrate concentration dependence of the pseudo-first-order rate constants for the oxidation of (■) CH_3OH, (□) CD_3OH, (●) CH_3OD and (○) CD_3OD at 10 °C in CD_3CN.
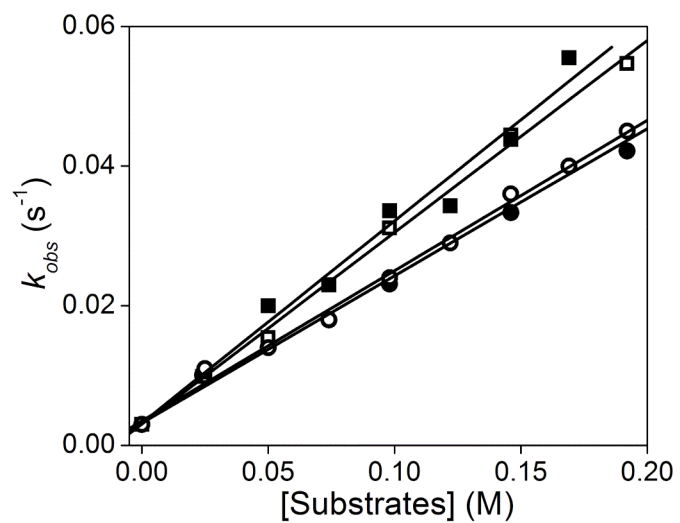
Fig. S5. Plots of the substrate concentration dependence of the pseudo-first-order rate constants for the oxidation of (■) *t*-BuOH, (□) *t*-BuOH-*d₉*, (●) *t*-BuOD and (○) *t*-BuOH-*d₁₀* at 10 °C in CD_3CN.

Table S1. Crystal data and structure refinement for [Fe$^{III}_2$O(L)$_2$](BPh$_4$)$_2$ (**1-BPh$_4$**). CCDC 711011 contains the supplementary crystallographic data. These data can be obtained free of charge from The Cambridge Crystallographic Data Centre via www.ccdc.cam.ac.uk/data_request/cif.

Formula	C$_{92}$H$_{102}$B$_2$Fe$_2$N$_8$O$_7$
Formula weight, amu	1565.14
Temperature, K	173(2)
Wavelength, Å	0.71073
Crystal system	Triclinic
Space group	P$_{-1}$
a, Å	12.8517(13)
b, Å	16.7315(17)
c, Å	21.303(2)
α, deg	78.353(2)
β, deg	75.198(2)
γ, deg	71.227(2)
Volume, Å^3	4157.1(7)
Z	2
Density (calculated), g/cm^3	1.250
Absorption coefficient, mm^{-1}	0.409
Completeness to θ = 25.06°	99.5%
Goodness-of-fit	1.354
Final *R* indices [*I* > 2δ(*I*)]	0.0452
R indices (all data)	0.0638

Table S2. EXAFS fitting results for **1**.[a]

	Fe-N/O			Fe-O/N			Fe•••Fe			Fe•••C			
fit	n	r	σ^2	n	r	σ^2	n	r	σ^2	n	r	σ^2	F^{b}
1	4	2.13	6.3										0.859
2	4	2.11	5.5	1	1.79	1.3							0.792
3	4	2.10	5.6	1	1.78	1.0	1	2.98	0.5				0.427[c]
4	4	2.10	5.6	1	1.78	1.1				8	3.00	1.1	0.404[c]
5	4	2.11	5.5	1	1.78	1.2	1	2.97	-0.1	4	3.08	0.1	0.331
6	4	2.11	5.5	1	1.78	1.2	1	2.97	0.2	5	3.07	1.7	0.333
7	*4*	*2.11*	*5.5*	*1*	*1.78*	*1.2*	*1*	*2.97*	*0.6*	*6*	*3.07*	*3.9*	*0.340*

[a] Fourier transform range k = 2.0 – 15.0 Å^{-1} (resolution = 0.121 Å). σ^2 is in units of 10^{-3} Å^2. All fits are to unfiltered data. The first shell was fit using scatterers with nitrogen parameters, while the second shell was fit with oxygen parameters; however, EXAFS cannot distinguish between backscatterers differing by Z = 1.

[b] Goodness-of-fit parameter F defined as $[\Sigma k^6(\chi_{exptl}-\chi_{calc})^2 / \Sigma k^6\chi_{exptl}^2]^{1/2}$.

[c] The outer-shell feature cannot be adequately fit using Fe•••Fe or Fe•••C shells alone. A combination of the two is required, and is supported by the X-ray crystal structure of this complex.

Table S3. EXAFS fitting results for **2**.[a]

	Fe-N/O			Fe-O/N			Fe•••Fe			Fe•••C			
fit	n	r	σ^2	n	r	σ^2	n	r	σ^2	n	r	σ^2	F^{b}
1	4	1.98	3.3										0.685
2	4	1.96	2.9	1	1.71	3.8							0.633
3	4	1.97	3.0	0.9	1.71	3.2							0.633
4	4	1.97	3.2	0.9	1.71	3.0	1	3.12	2.7				0.641
5	4	1.97	3.2	0.9	1.71	2.9	0.9	3.11	2.0				0.631
6	4	1.96	3.5	0.9	1.70	2.8				3	2.87	-0.6	0.484[c]
7	4	1.96	3.4	0.9	1.70	2.8				4	2.87	0.4	0.491[c]
8	4	1.96	3.3	0.9	1.70	2.8				5	2.87	1.3	0.506[c]
9	4	1.97	3.6	0.9	1.70	2.8	0.9	3.06	6.5	3	2.88	-0.9	0.471
10	4	1.97	3.5	0.9	1.70	2.7	0.9	3.07	4.6	4	2.88	0.0	0.466
11	*4*	*1.96*	*3.5*	*0.9*	*1.70*	*2.7*	*0.9*	*3.07*	*3.6*	*5*	*2.89*	*0.9*	*0.468*
12	4	1.96	3.5	0.9	1.70	2.6	0.9	3.08	2.7	6	2.89	1.9	0.476

[a] Fourier transform range k = 2.0 – 14.9 Å^{-1} (resolution = 0.122 Å). σ^2 is in units of 10^{-3} Å^2. All fits are to unfiltered data. The first shell was fit using scatterers with nitrogen parameters, while the second shell was fit with oxygen parameters; however, EXAFS cannot distinguish between backscatterers differing by Z = 1. The value of n for the Fe-O/N and Fe•••Fe shells was fixed at 0.9 in view of the fact that the sample was determined to contain 90% **2** by UV-vis spectroscopy.

[b] Goodness-of-fit parameter F defined as $[\Sigma k^6(\chi_{exptl}-\chi_{calc})^2 / \Sigma k^6\chi_{exptl}^2]^{1/2}$.

[c] We assign the shell at 2.87 Å to Fe•••C scatterers by analogy to previous studies on other low-spin iron complexes with pyridine ligands.

Table S4. EXAFS fitting results for **3**.[a]

	Fe-N/O			Fe-O/N			Fe•••Fe			Fe•••C			
fit	n	r	σ^2	n	r	σ^2	n	r	σ^2	n	r	σ^2	F[b]
1	4	1.97	4.0										0.515
2	5	1.97	5.8										0.557
3	4	1.97	3.3	1	1.73	7.8							0.497
4	4	1.97	3.4	0.8	1.72	5.8							0.495
5	5	1.96	4.8	1	1.70	4.9							0.509
6	5	1.96	5.0	0.8	1.70	3.3							0.506
7	4	1.96	3.4	0.8	1.72	5.7	1	3.12	3.9				0.492
8	4	1.96	3.4	0.8	1.72	5.6	0.8	3.12	2.4				0.471
9	4	1.96	3.6	0.8	1.71	5.4				2	2.87	-1.2	0.351[c]
10	4	1.96	3.6	0.8	1.71	5.2				3	2.87	0.2	0.359[c]
11	4	1.96	3.5	0.8	1.71	5.0				4	2.87	1.4	0.379[c]
12	4	1.96	3.6	0.8	1.71	5.4	0.8	2.86	4.0	2	3.12	-0.8	0.322
13	4	1.96	3.6	0.8	1.71	5.3	0.8	3.08	4.9	3	2.88	0.2	0.316
14	*4*	*1.96*	*3.6*	*0.8*	*1.71*	*5.2*	*0.8*	*3.08*	*3.9*	*4*	*2.88*	*1.5*	*0.318*

[a] Fourier transform range k = 2.0 – 15.0 Å^{-1} (resolution = 0.121 Å). σ^2 is in units of 10^{-3} Å^2. All fits are to unfiltered data. The first shell was fit using scatterers with nitrogen parameters, while the second shell was fit with oxygen parameters; however, EXAFS cannot distinguish between backscatterers differing by Z = 1. The value of n for the Fe-O/N and Fe•••Fe shells was fixed at 0.8 in view of the fact that the sample was determined to contain 80% **3** by UV-vis spectroscopy.

[b] Goodness-of-fit parameter F defined as $[\Sigma k^6(\chi_{exptl}-\chi_{calc})^2 / \Sigma k^6\chi_{exptl}^2]^{1/2}$.

[c] We assign the shell at 2.87 Å to Fe•••C scatterers by analogy to previous studies on other low-spin iron complexes with pyridine ligands.

Table. S5. Summary of kinetic data of the reaction of **3** with substrates under anaerobic conditions at 10 °C in CD_3CN.

Substrate	BDE[a] in kcal/mol (number of equivalent X-H bonds that react with **3**)		$k_2{}^{[b]}$ ($M^{-1} \cdot s^{-1}$)	KIE
	C-H	O-H		
THF	92.1(4)		0.13	3.0
THF-d_4			0.043	
c-C$_8$H$_{16}$	95.7(16)		0.22	
t-BME	96.1(3)		0.045	
CH$_3$CN	97(3)		0.014	
c-C$_6$H$_{12}$	99.3(12)		0.081	3.5
c-C$_6$D$_{12}$			0.023	
CH$_3$OH	96.1(3)	105.2(1)	0.14	1.5
CH$_3$OD			0.094	
CD$_3$OH			0.13	1.5
CD$_3$OD			0.084	
$tert$-C$_4$H$_9$OH	100(9)	106.3(1)	0.30	1.4
$tert$-C$_4$H$_9$OD			0.21	
$tert$-C$_4$D$_9$OH			0.28	1.4
$tert$-C$_4$D$_9$OD			0.20	

[a] D_{X-H} values were obtained from refs 7-9.

[b] The k_2' values used in Fig. 5 were determined by dividing k_2 values listed here by the number of equivalent H-atoms on the substrate listed in the BDE column.

Table. S6. Summary of product analysis results of the reaction of **3** with c-C_6H_{12}, c-C_6H_{10} and c-C_6H_8 under anaerobic conditions at 10 °C in CD_3CN.

Substrate	[Fe^{III}OFe^{III}]	Equiv of 3 formed	c-C_6H_{10} formed	c-C_6H_8 formed	C_6H_6 formed	Oxidizing equiv used
c-C_6H_{12} 100 mM	1 mM	0.7	0.10	0.06	–	0.44 (63%)
	1 mM	0.8	0.10	0.08	–	0.52 (65%)
	1 mM	0.9	0.12	0.08	–	0.56 (62%)
c-C_6H_{10} 2 mM	1 mM	0.8	–	0.36	–	0.72 (90%)
c-C_6H_{10} 5 mM	1 mM	0.8	–	0.35	–	0.70 (88%)
c-C_6H_{10} 10 mM	1 mM	0.8	–	0.40	–	0.80 (100%)
c-C_6H_8 2 mM	1 mM	0.8	–	–	0.36	0.72 (90%)
c-C_6H_8 5 mM	1 mM	0.8	–	–	0.34	0.68 (85%)
c-C_6H_8 10 mM	1 mM	0.8	–	–	0.38	0.76 (95%)

Table. S7. Summary of product analysis results of the reaction of **3** with *tert*-butanol under anaerobic conditions at 10 °C in CD_3CN.

[t-BuOH] (mM)	Acetone	2-methylpropene	Oxidation equivalents used (80% diiron(IV) yield assumed)
50	30%	50%	38%
100	37%	23%	46%
250	40%	39%	50%
400	45%	25%	56%
500	39%	30%	49%

References

1.   Schatz, M. *et al.* Syntheses and characterization of copper complexes of the ligand (2-aminoethyl)bis(2-pyridylmethyl)amine (uns-penp) and derivatives. *Dalton Trans.*, 1480-1487 (2003).
2.   Hagen, K.S. Iron(II) Triflate Salts as Convenient Substitutes for Perchlorate Salts: Crystal Structures of $[Fe(H_2O)_6](CF_3SO_3)_2$ and $Fe(MeCN)_4(CF_3SO_3)_2$. *Inorg. Chem.* **39**, 5867-5869 (2000).
3.   George, G.N. (Stanford Synchrotron Radiation Laboratory, Stanford Linear Accelerator Center, Stanford; 2000).
4.   Klinker, E.J. *et al.* A Tosylimido Analogue of a Nonheme Oxoiron(IV) Complex *Angew. Chem. Int. Ed.* **45**, 7394-7397 (2006).
5.   Scarrow, R.C. *et al.* X-ray Spectroscopy of the Iron Site of Soybean Lipoxygenase-1: Changes in Coordination upon Oxidation or Addition of Methanol. *Biochemistry* **33**, 15023-15035 (1994).
6.   Rohde, J.-U. *et al.* Structural Insights into Nonheme Alkylperoxoiron(III) and Oxoiron(IV) Intermediates by X-ray Absorption Spectroscopy. *J. Am. Chem. Soc.* **126**, 16750-16761 (2004).
7.   Luo, Y.-R. BDEs of O-X bonds, in *Comprehensive Handbook of Chemical Bond Energies* 255-369 (Taylor & Francis, Boca Raton; 2007).
8.   Luo, Y.-R. BDEs of C-H bonds, in *Comprehensive Handbook of Chemical Bond Energies* 19-147 (Taylor & Francis, Boca Raton; 2007).
9.   Kaizer, J. *et al.* Nonheme Fe^{IV}O Complexes That Can Oxidize the C-H Bonds of Cyclohexane at Room Temperature. *J. Am. Chem. Soc* **126**, 472-473 (2004).